



**HAL**  
open science

## Thermodynamic Study of binary and ternary systems containing CO<sub>2</sub> + impurities in the context of CO<sub>2</sub> transportation

Christophe Coquelet, Alain Valtz, Philippe Arpentinier

► **To cite this version:**

Christophe Coquelet, Alain Valtz, Philippe Arpentinier. Thermodynamic Study of binary and ternary systems containing CO<sub>2</sub> + impurities in the context of CO<sub>2</sub> transportation. *Fluid Phase Equilibria*, 2014, 382, pp.205-211. 10.1016/j.fluid.2014.08.031 . hal-01067191

**HAL Id: hal-01067191**

**<https://minesparis-psl.hal.science/hal-01067191>**

Submitted on 28 Jan 2016

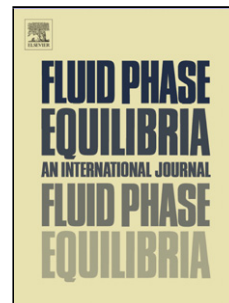
**HAL** is a multi-disciplinary open access archive for the deposit and dissemination of scientific research documents, whether they are published or not. The documents may come from teaching and research institutions in France or abroad, or from public or private research centers.

L'archive ouverte pluridisciplinaire **HAL**, est destinée au dépôt et à la diffusion de documents scientifiques de niveau recherche, publiés ou non, émanant des établissements d'enseignement et de recherche français ou étrangers, des laboratoires publics ou privés.

## Accepted Manuscript

Title: Thermodynamic Study of binary and ternary systems containing CO<sub>2</sub> + impurities in the context of CO<sub>2</sub> transportation

Author: C. Coquelet A. Valtz P. Arpentinier



PII: S0378-3812(14)00488-9  
DOI: <http://dx.doi.org/doi:10.1016/j.fluid.2014.08.031>  
Reference: FLUID 10247

To appear in: *Fluid Phase Equilibria*

Received date: 21-4-2014  
Revised date: 26-8-2014  
Accepted date: 27-8-2014

Please cite this article as: C.Coquelet, A.Valtz, P.Arpentinier, Thermodynamic Study of binary and ternary systems containing CO<sub>2</sub> + impurities in the context of CO<sub>2</sub> transportation, Fluid Phase Equilibria <http://dx.doi.org/10.1016/j.fluid.2014.08.031>

This is a PDF file of an unedited manuscript that has been accepted for publication. As a service to our customers we are providing this early version of the manuscript. The manuscript will undergo copyediting, typesetting, and review of the resulting proof before it is published in its final form. Please note that during the production process errors may be discovered which could affect the content, and all legal disclaimers that apply to the journal pertain.

Thermodynamic Study of binary and ternary systems containing CO<sub>2</sub> +  
impurities in the context of CO<sub>2</sub> transportation

C. Coquelet<sup>a\*</sup>, A. Valtz<sup>a</sup>, P. Arpentinier<sup>b\*</sup>

<sup>a</sup> MINES ParisTech, PSL Research University, CTP-Centre Thermodynamic of Processes 35,  
Rue Saint Honoré, 77305 Fontainebleau, France

<sup>b</sup> Air Liquide Centre de Recherche Claude Delorme 1, chemin de la porte des Loges BP 126,  
78354 Loges en Josas, France

\*Corresponding authors:

E-mail: christophe.coquelet@mines-paristech.fr Telephone: (33) 164694962. Fax (33) 164694968.

E-mail: Philippe.Arpentinier@airliquide.com Telephone: (33)139076283. Fax (33) 139561122.

### Highlights

We determine new experimental data concerning CO<sub>2</sub> + SO<sub>2</sub>, CO<sub>2</sub> + NO binary systems and  
CO<sub>2</sub> + O<sub>2</sub> + Ar, CO<sub>2</sub> + SO<sub>2</sub> + O<sub>2</sub> Ternary systems

An equipment based on “static analytic” method with phase sampling.

Cubic equation of state is used for the data treatment.

Data and model are used to generate complete phase diagram of the different systems

CO<sub>2</sub> capture transportation and storage, or CO<sub>2</sub> capture transportation and utilization, are two  
ways which should be considered in the industry in order to reduce the emission of CO<sub>2</sub>. After  
capture, CO<sub>2</sub> is not pure and contains impurities like SO<sub>2</sub>, NO<sub>x</sub>, N<sub>2</sub>, O<sub>2</sub> and Ar for example.  
Two binary systems involving CO<sub>2</sub> were studied in this work (CO<sub>2</sub> + SO<sub>2</sub> at 263.15 and

333.21 K and between 0.1 and 8.8 MPa and CO<sub>2</sub> + NO in at 232.93, 252.98 and 273.15 K, and between 1 and 11.5 MPa ) and two ternary systems (CO<sub>2</sub> + O<sub>2</sub> + Ar and CO<sub>2</sub> + SO<sub>2</sub> + O<sub>2</sub> (expected composition (0.94/0.03/0.03 mole fractions)) at 253, 273 and 293 K, between 1.9 and 7.6 MPa) were also studied experimentally. The equipment used is based on “static-analytic” method, taking advantage of two capillary samplers (Rolsi™, Armines' patent). The classical Peng-Robinson equation of state is used to represent the isothermal  $P$ ,  $x$ ,  $y$  data..

*Keywords:* VLE data, High-pressures, modeling, Phase diagram determination, carbon dioxide, impurities.

### List of symbols:

$A$	Helmholtz energy [J.mol <sup>-1</sup> ]
$F$	Objective function
$k_{ij}$	Binary interaction parameter between specie $i$ and specie $j$
$P$	Pressure [MPa]
$T$	Temperature [K]
$x$	Liquid mole fraction
$y$	Vapor mole fraction

### Greek letters

$\mu$	Chemical potential [J.mol <sup>-1</sup> ]
$\Delta n_i$	Variation of $n_i$

### Superscript

°	Reference state
---	-----------------

### Subscripts

$C$	Critical property
$cal$	Calculated property
$exp$	Experimental property
$i,j$	Molecular species
$\infty$	Infinite pressure reference state
Bub	Bubble point
Dew	Dew point

### Introduction

CO<sub>2</sub> is one of the greenhouse gases responsible of global climate change. Human activities and particularly industries are mainly responsible of its emission. In order to solve the

problem of green house gas emission in the context of energy production, one solution consists to capture the CO<sub>2</sub> emissions and to transport it to storage location. Concerning the CO<sub>2</sub> capture, three main processes are generally used: post-combustion where CO<sub>2</sub> is captured after the energy production step, pre-combustion where CO<sub>2</sub> is captured before the energy production step and oxy-combustion where pure oxygen is used during the energy production step in order to facilitate the CO<sub>2</sub> capture. Several technologies for the CO<sub>2</sub> capture depending on the composition of the CO<sub>2</sub> (the stream after combustion is mainly composed of N<sub>2</sub> and CO<sub>2</sub>) are available. One can use chemical or physical solvents (absorption), or cryogenic processes, or adsorption on porous media or membranes (Lecomte et al. [1]). At the outlet of such processes, the stream is very rich in CO<sub>2</sub> but some impurities are also present and their compositions may vary between 0.1 and 5 %. The transport of CO<sub>2</sub> rich stream is done using pipeline or ship. The presence of the impurities may modify the phase diagram of the stream. The figure 1 (extract from Li [2]) illustrates the different thermodynamic conditions regarding CO<sub>2</sub> transportation and storage. Also from Li et al. [3], the main conditions of transportation are  $0.5 < P < 20$  MPa and  $218.15 < T < 303.15$  K.

As indicated, the conditions of temperature and pressure for the transportation are different if we consider the pipeline or the ship solutions.

During the transportation of CO<sub>2</sub>, in each case, it is important to know the thermodynamic behaviors in the presence of water (possibility of water condensation and so corrosion with CO<sub>2</sub> and/or the impurities, or blockage due to gas hydrate formation) and to understand the role played by impurities which are heavier (NO<sub>2</sub>, SO<sub>2</sub>, H<sub>2</sub>S) or lighter (Ar, O<sub>2</sub>, N<sub>2</sub>, CO, NO, NO<sub>2</sub>, N<sub>2</sub>O) than the CO<sub>2</sub>. Li et al. [3] have also noticed a lack of experimental data regarding vapor liquid equilibrium properties and densities.

In case of problem during the transportation, for example a leakage, the presence of the impurities may lead to the apparition of vapor-liquid equilibrium if the condition of temperature and pressure are favorable. Consequently, the conditions of flow must be changed leading thus to increase the cost of fluid transportation. Also, the viscosity may also change in the presence of the impurities and so have a non negligible role in the cost of CO<sub>2</sub> transportation.

In this paper we will present new experimental data regarding two binary system (CO<sub>2</sub> + NO, CO<sub>2</sub> + SO<sub>2</sub>) and two ternary systems (CO<sub>2</sub> + O<sub>2</sub> + Ar and CO<sub>2</sub> + SO<sub>2</sub> + O<sub>2</sub>). Concerning the composition of the two ternary systems, they are rich in CO<sub>2</sub>, i.e.  $z_{\text{CO}_2} > 0.95$ . The technique used to obtain the data is based on static-analytic method. The equipment is identical to the one used for the study of CO<sub>2</sub> + Ar or CO<sub>2</sub> + H<sub>2</sub>S binary system (Coquelet et al. [4], Chapoy et al. [5]).

The classical Peng Robinson Equations of State [6] (PR EoS) commonly used in industry is used to correlate the data and determined binary interaction parameters (BIP). The authors have used Simulis Thermodynamic® software from Prosim, France. Literature data will be used for the determination of BIP of the SO<sub>2</sub> + O<sub>2</sub>, CO<sub>2</sub> + O<sub>2</sub>, O<sub>2</sub> + Ar and CO<sub>2</sub> + Ar binary systems. According to van Konynenburg and Scott classification [7], all of these systems are classified as type I or II.

## Experimental Section

All the details concerning the chemicals used are presented in Table 1.

The apparatus used in this work is based on a static-analytic method with liquid and vapor phase sampling. This apparatus is identical to the one described by Coquelet et al. [4]. The volume of the equilibrium cell is around 28 cm<sup>3</sup>. The equilibrium cell is immersed inside a

regulated liquid bath. Temperatures are measured with two platinum resistance thermometer probes (Pt100) inserted inside walls of the equilibrium cell. These Pt100 probes are calibrated against a 25  $\Omega$  reference probe (TINSLEY Precision Instrument) certified by the Laboratoire National d'Essais (Paris) following the International Temperature Scale 1990 protocol.

Pressures are measured using a pressure transducer (Druck, type PTX611, range: 0 - 20 MPa). This sensor is calibrated against a dead weight pressure balance (5202S model from Desgranges & Huot). For the low pressure measurement, another pressure transducer (Druck, type PTX611, range: 0 – 1.6 MPa) was used. Pressure and temperature data acquisition is performed with a computer linked to a data acquisition unit (Hewlett Packard HP34970A). The resulting expanding uncertainties in this work are  $\pm 0.02$  K ( $k=2$ ),  $\pm 0.002$  MPa ( $k=2$ ) for the high pressure transducer and  $\pm 0.0002$  MPa ( $k=2$ ) for the low pressure transducer.

The analytical work was carried out using a gas chromatograph (VARIAN model CP-3800) equipped with a thermal conductivity detector (TCD) connected to a data acquisition system (BORWIN ver 1.5, from JMBS). The analytical column is Porapak Q 80/100 Mesh, 2m  $\times$  1/8 Silcosteel from RESTECK, France. The TCD was repeatedly calibrated by introducing known amounts of each pure compound through a syringe in the injector of the gas chromatograph. Taking into account the uncertainties due to calibrations, resulting absolute uncertainties on vapor and liquid mole fractions are less than  $u(x)=0.002$  for NO + CO<sub>2</sub> and less than  $u(x)=0.006$  for CO<sub>2</sub> + SO<sub>2</sub> binary systems.

Concerning the two ternary systems, the same equipment with the same technique was used. The uncertainties for the compositions CO<sub>2</sub>+SO<sub>2</sub>+O<sub>2</sub> and CO<sub>2</sub>+O<sub>2</sub>+Ar are less than  $u(x)=0.005$  and  $u(x)=0.002$  respectively.

### C) Procedures

#### -Binary systems

At room temperature, the equilibrium cell and its loading lines are evacuated down to 0.1 Pa. The cell is first loaded with the heaviest component (about 5 cm<sup>3</sup>). Then the cell is

immersed into the liquid bath. Equilibrium temperature is assumed to be reached when the two Pt100 probes (one located at top of equilibrium cell, the other in the bottom) give equivalent temperature values within experimental uncertainty for at least 5 minutes. After recording the vapor pressure of the heavier component at equilibrium temperature, the lighter component is then introduced step by step, leading to successive equilibrium mixtures of increasing overall lighter component content. Bubble and dew point curves are described with generally much more than eight P, x, y data (in liquid and vapor). Equilibrium is assumed to be reached when the total pressure remains unchanged within  $\pm 1.0$  kPa during a period of 10 min under efficient stirring.

For each equilibrium condition, at least five samples of both vapor and liquid phases are withdrawn using the capillary samplers (ROLSI<sup>TM</sup>), Armines's Patent, and analyzed in order to check for measurements repeatability.

#### **-Ternary systems**

The procedure is slightly different. Each pure component is introduced in their respective isothermal press of well known volume. A mixture of each ternary system is prepared and knowing the volumetric properties of each pure component and the variation of pressure of each isothermal press, the global composition is determined. Table 2 resumes the composition of the two ternary systems.

The experimental procedure consists to load at a given temperature the mixture in order to reach the expected pressure. Like with binary system, equilibrium is assumed to be reached when the total pressure remains unchanged within  $\pm 1.0$  kPa during a period of 10 min under efficient stirring. Also, for each equilibrium condition, at least five samples of both vapor and liquid phases are withdrawn using the capillary samplers ROLSI<sup>TM</sup> and analyzed in order to check for measurements repeatability.



## Correlations

The critical temperatures ( $T_C$ ), critical pressures ( $P_C$ ), and acentric factors ( $\omega$ ), for each pure components are provided in Table 3 and are from Reid et al. [8].

Our experimental VLE data are correlated by means of Simulis Thermodynamics software developed by PROSIM SA, France. The classical PR EoS is used. The binary interaction parameter  $k_{ij}$  is adjusted directly onto VLE data through a modified Simplex type algorithm using the following objective function:

$$F = \frac{100}{N} \left[ \sum_1^N \left( \frac{P_{dew\ exp} - P_{dew\ cal}}{P_{dew\ exp}} \right)^2 + \sum_1^N \left( \frac{P_{bub\ exp} - P_{bub\ cal}}{P_{bub\ exp}} \right)^2 \right] \quad (1)$$

Where  $N$  is the number of data points,  $P_{exp}$  and  $P_{cal}$  are respectively the measured and calculated pressure, dew and bubble correspond to dew and bubble points calculations.

The deviation, AADU (Average Absolute Deviation), and the BIASU, applied on liquid and vapor phase mole fractions, are defined by:

$$AADU = (100/N) \sum | (U_{cal} - U_{exp}) / U_{exp} | \quad (2)$$

$$BIASU = (100/N) \sum ( (U_{exp} - U_{cal}) / U_{exp} ) \quad (3)$$

where  $N$  is the number of data points, and  $U = p, x_i$  or  $y_i$ .

These indicators give information about the agreement between model and experimental results. They are calculated in each table of results.

Procedures to calculate critical points were proposed by Heidemann and Khalil [9] in 1980 and Michelsen and Heidemann [10] in 1981. They assumed that the stability criterion for an isothermal variation (between an initial state, stable and a very close new one) can be explained with a minimum of the Helmholtz energy (Eq. 4). They have also considered that the volume variation at the critical point is constant ( $\Delta V = V - V^0 = 0$ )

$$A - A^0 + P^0(V - V^0) - \sum_i \mu_i^0 (n_i - n_i^0) = A - A^0 - \sum_i \mu_i^0 \Delta n_i \geq 0 \quad (4)$$

The method starts from the Taylor series expansion of the Helmholtz energy  $A$  around the stable state at constant total volume  $V$  (equation 5).

$$\frac{1}{2} \sum_i \sum_j \left( \frac{\partial^2 A}{\partial n_i \partial n_j} \right)_{T,V} \Delta n_i \Delta n_j + \frac{1}{6} \sum_i \sum_j \sum_k \left( \frac{\partial^3 A}{\partial n_i \partial n_j \partial n_k} \right)_{T,V} \Delta n_i \Delta n_j \Delta n_k + \text{Residual term} > 0 \quad (5)$$

The critical point corresponds to the limit of stability. They developed an algorithm to calculate the critical point with a van der Waals type EoS, combined with the classical mixing rules. The method consists of the resolution of the following system of equations (6-8) into two inner and outer loops (more details are given in the original paper). With equation 7, the critical temperature is obtained at given global composition and volume. The first part of equation 5 is a matrix positive semidefinite (eq 6) and its determinant is equal to zero (eq 7) at the critical point.

$$Q\Delta N = 0 \text{ with } \Delta N^T \Delta N = 1 \quad (6)$$

$$\det(Q) = 0 \text{ with } Q \text{ the matrix of } q_{ij} = \left( \frac{\partial^2 A}{\partial n_i \partial n_j} \right)_{T,V} \quad (7)$$

The vector  $\Delta N$  is then obtained considering the equation 6. This vector corresponds to the vector of mole number with elements  $\Delta n_i$ .

And with the values of  $\Delta n_i$  obtained, we can determine the critical volume.

$$C = \sum_i \sum_j \sum_k \left( \frac{\partial^3 A}{\partial n_i \partial n_j \partial n_k} \right)_{T,V} \Delta n_i \Delta n_j \Delta n_k = 0 \quad (8)$$

Critical pressure is determined using the selected model at a given composition.

## Results and discussion:

### A) $CO_2$ $SO_2$ binary system

This system was the topic of a previous paper published by Lachet et al. [11] but the data were not presented. The authors have found two sets of data in the literature: the data from the thesis of Caubet [12] and the data from Thiel and Shulte [13]. The data of Thiel and Shulte cannot be used for the data treatment (there are only two equilibrium points measured at

atmospheric pressure) and the data of Caubet correspond to dew and bubble point measurements. We have used corresponding objective function for the data treatment. The Table 4 presents the results of our treatment. Regarding the deviations considering bubble point calculation, we have considered for the rest of the study no temperature dependency. In reality, temperature dependency does not improve significantly the data treatment and so the prediction of the phase diagram. Concerning the literature data, the range of temperature is from 295 to 418 K. If we consider our BIP value, the prediction of literature data gives AAD=6.3% with a maximum at 30%. The data treatment of literature data with no temperature dependency gives  $k_{ij}=0.078$  with AAD=5.6%. Of course, close to the mixture critical point the model fails to represent the data. The figure 2 presents the phase diagram. The BIP is given in Table 5. There are disagreements between the data of Caubet and ours. The data of Caubet [12] were used to compare critical point prediction and we can see that he observed critical point in VLE region. In comparison with the calculations we have done using our model, we can see that deviations increase when the composition of the mixture become richer in CO<sub>2</sub> (figure 2).

#### *B) NO CO<sub>2</sub> binary system*

From the knowledge of the authors, no literature data concerning this system are available. The new data were determined at 3 temperatures 273.02, 252.98 and 232.93 K. The Table 6 presents our experimental results. Our data were correlated with the same model used for CO<sub>2</sub> + SO<sub>2</sub> binary system. Table 7 presents the BIP obtained at each temperature and also with no temperature dependency. Figure 3 presents the phase diagram. As we can see, the BIP is dependent of the temperature, but we can see that using a temperature independent parameter the deviations are not very different. For this reason we have considered  $k_{ij} = 0.0323$  (see table 7) for the rest of the study. Moreover, the model fails to calculate the VLE in the region close to the mixture critical point. In order to improve the representation of VLE

properties close to the mixture critical point, it is necessary to select a mixing rule with more BIPs. We have also calculated the critical line of this binary system (locus made up by all the mixture critical points of the binary system). As the melting point of CO<sub>2</sub> is equal to 216.58 K, we have decided to stop the prediction at  $x_1=0.77$  ( $T_C=216.57$  K) because we have no information concerning the thermodynamic behaviour of the system in the presence of solid phase.

### *C) Ternary mixture*

Tables 8 and 9 presented the results we have obtained for the two ternary mixtures. The data treatment of the data is using the PR EoS. We have used the BIP obtained from the data treatment of each binary mixture of the considered ternary system. Concerning the binary system CO<sub>2</sub> + Ar, we have used the data from Coquelet et al. [4] (from 233.32 and 299.21 K). We have considered BIP not dependent on temperature. The  $k_{ij}$  value obtained is equal to 0.1053 and AAD=4.1% (Table 10). The data close to the mixture critical point are badly calculated with the selected model. For Ar + O<sub>2</sub> binary system, we have considered the data of Baba-Ahmed et al. [14] (from 101.8 to 123.17 K). Like CO<sub>2</sub> + Ar, the BIP is independent of temperature. The  $k_{ij}$  value obtained is equal to 0.0126 and AAD= 0.3% (Table 10). For CO<sub>2</sub>+ O<sub>2</sub> binary system, we have found 5 references in the literature (Fredenslund and Sather [15], Muirbrook and Prausnitz [16], Kaminishi and Toriumi [17], Zenner and Danna [18] and Keesom [19]). The data from Keesom were not used because they correspond to measurements done for pressure lower than atmospheric pressure. The VLE were measured from 218.15 to 298.15 K. Like the other systems, the BIP is independent of the temperature. The  $k_{ij}$  value obtained is equal to 0.1053 and AAD= 4.7% (Table 10). We can notice that we have obtained after treatment roughly the same  $k_{ij}$  values and deviations for CO<sub>2</sub> + O<sub>2</sub> and CO<sub>2</sub> + Ar binary systems. For the SO<sub>2</sub> + O<sub>2</sub> binary system, we have used previous published

data (El Ahmar et al. [20]) and fitted BIP considering no temperature dependency. We have used the VLE data measured at 323.15 and 343.15 K which are the lowest temperature. The BIP value obtained is 0.2336 with AAD= 4.5 % (Table 10). Moreover Dornte and Fergusson [21] have published some data at atmospheric pressure. Regarding the range of pressure, these data cannot be used.

We have used our thermodynamic model with the respective BIP fitted on our and literature data. First we have considered a Flash algorithm (because global compositions were given) to compare our experimental data (mixture 1: CO<sub>2</sub>(1) + Ar (2) + O<sub>2</sub> (3); mixture 2: O<sub>2</sub>(1) + CO<sub>2</sub>(2) + SO<sub>2</sub>(3)) and prediction using our model with the BIP determined in this study. Table 11 presents the deviations. Figure 4 presents the PT envelop of the two mixtures. As can be seen, our model predicts satisfactory the thermodynamic behavior of the two mixtures.

### **Conclusion.**

New experimental data concerning two binary systems were determined using equipment which technique is based on static analytic method. The equipment takes advantage of two capillary samplers (ROLSI<sup>TM</sup> connected to gas chromatograph. The same technique was used for the determination of VLE properties of two ternary mixtures rich in CO<sub>2</sub>. We have used classical Peng-Robinson equation of state and determined binary interaction parameters. The model defined predicts very well the VLE properties of the two ternary mixtures.

### **Acknowledgments**

Philippe Arpentinier gratefully acknowledges ANR for the funding of the project “Trans CO<sub>2</sub>”. Christophe Coquelet and Alain Valtz are very grateful to Air Liquide for the partnership. Christophe Coquelet would also like to acknowledge institute CARNOT MINES.

**References**

- [1] F. Lecomte, P. Broutin et E. Lebas. Le captage du CO<sub>2</sub> : des technologies pour réduire les émissions de gaz à effet de serre Editions Technip 2010, ISBN 978-2-7108-0938-8
- [2] H. Li Thermodynamic properties of CO<sub>2</sub> mixtures and their applications in advanced power cycles with CO<sub>2</sub> capture processes PhD thesis RIT Stockholm, Sweden
- [3] H. Li, J.P. Jakosen, O. Wilhelmsen, J. Yan Applied Energy 88 (2011) 3567-3579.
- [4] C. Coquelet, A. Valtz, F. Dieu, D. Richon, P. Arpentinier, F. Lockwood Fluid Phase Equilib. 273 (2008) 38-43
- [5] A. Chapoy, C. Coquelet, H. Liu, A. Valtz, B. Tohidi, Fluid Phase Equilibria 356 (2013) 223-228
- [6] D.Y. Peng, D.B. Robinson, Ind. Eng. Chem. Fundam. 15 (1976) 59-64.
- [7] P.H. van Konynenburg and R.L. Scott, Philos. Trans. R. Soc., 298 (1980) 495-539
- [8] R.C. Reid, J.M. Prausnitz, B.E. Poling, the properties of gases and liquids, fourth edition, McGraw-Hill Book Company, 1987.
- [9] R. A. Heidemann, A. M. Khalil, AIChE J. 26 (1980) 769-779.
- [10] M. L. Michelsen, R.A. Heidemann, AIChE J. 27 (1981) 521-523.
- [11] V. Lachet, T. de Bruin, P. Ungerer, C. Coquelet, A. Valtz, V. Hasanov, F. Lockwood, D. Richon, Energy Procedia 1 (2009) 1641-1647.
- [12] M. F. Caubet, Liquéfaction des mélanges gazeux. Université de Bordeaux Thesis, 1901
- [13] A. Thiel et E. Schulte Z. Phys. Chem. 96 (1920) 312-342.
- [14] A. Baba Ahmed, Appareillage pour l'étude des équilibre liquide – vapeur dans le domaine cryogénique conception et développement, thèse Ecole des Mines de Paris, 1999.
- [15] A. A. Fredenslund and G. A. Sather J. Chem. Eng. Data 15 (1970) 17-22.
- [16] N. K. Muirbrook and J. M. Prausnitz AIChE J. 11 (1965) 1092-1102.
- [17] G.I. Kaminishi and T. Toriumi Kogyo Kagaku Zasshi, 69 (1966) 175.
- [18] G. H. Zenner and L. I. Dana Chem. Eng. Progr. Symp. Ser., 44 (1963) 36-41.
- [19] W.H. Keesom Comm.Phys.Lab.Univ.Leiden, 88 (1903) 1.
- [20] E. El Ahmar, B. Creton, A. Valtz, C. Coquelet, V. Lachet, D. Richon, P. Ungerer Fluid Phase Equilib. 304 (2011) 21-34.
- [21] Dornte R.W. and Ferguson C.V., Ind. Eng. Chem., 31 (1939) 112.

## List of figures

Figure 1 : CO<sub>2</sub> phase diagram and applications. Figure extracted from Li [2].

Figure 2: Pressure composition phase diagram of the CO<sub>2</sub> (1) + SO<sub>2</sub> (2) binary system. (▲) 333.15 K, (●): 263.15 K. (×): experimental critical point from [12]. Solid lines: calculated using PR model with  $k_{ij}=0.0274$ , dashed line: corresponding mixture critical point line.

Figure 3: Pressure composition phase diagram of the NO (1) + CO<sub>2</sub> (2) binary system. (▲) 232.93 K, (●): 252.98 K. (■): 273.02 K Solid lines: calculated using PR model with  $k_{ij}=-0.0323$ , dashed line: corresponding mixture critical point line.

Figure 4: PT envelops of mixture 1 (solid line, CO<sub>2</sub> + O<sub>2</sub> + Ar (0.94/0.03/0.03)) and mixture 2 (dashed line, CO<sub>2</sub> + O<sub>2</sub> + SO<sub>2</sub> (0.94/0.03/0.03)). (Δ): predicted mixture 1 critical point, (●): predicted mixture 2 critical point ; (▲), experimental PT data of mixture 1 ; (×), experimental PT data of mixture 2.

## List of Tables

Table 1: Chemicals sample table

Table 2: Compositions of the two ternary systems study.

Table 3: Critical Properties of Pure Compounds from Reid at al. [8].

Table 4: Vapour–liquid<sup>a</sup> equilibrium pressures and phase compositions for CO<sub>2</sub> (1) - SO<sub>2</sub> (2) mixtures ( $\sigma$ : Standard deviation between samples; n: number of samples).

Table 5: Adjusted values of binary interaction parameters of CO<sub>2</sub> (1) + SO<sub>2</sub> (2) binary system and deviations.

Table 6: Vapour–liquid<sup>a</sup> equilibrium pressures and phase compositions for NO (1) - CO<sub>2</sub> (2) mixtures ( $\sigma$ : Standard deviation between samples; n: number of samples).

Table 7: Adjusted values of binary interaction parameters of NO (1) + CO<sub>2</sub> (2) binary system and deviations.

Table 8: Vapour–liquid<sup>a</sup> equilibrium pressures and phase compositions for CO<sub>2</sub> (1) + Ar (2) + O<sub>2</sub> (3) (mixture 2, 0.9366/0.0316/0.0318) mixtures ( $\sigma$ : Standard deviation between samples; n: number of samples).

Table 9: Vapour–liquid<sup>a</sup> equilibrium pressures and phase compositions for O<sub>2</sub> (1) - CO<sub>2</sub> (2) + SO<sub>2</sub> (3) (mixture 2, 0.0283/0.9205/0.0512) mixtures ( $\sigma$ : Standard deviation between samples; n: number of samples).

Table 10: Data treatment of literature data using PR EoS (BIP and deviations using bubble point calculation).

Table 11: Ternary systems: deviations between experimental and predicted values.

Table 1: Chemicals sample table.

Chemical	Source	Initial Mole	Purification	Final Mole	Analysis
Name		Fraction	Method	Fraction	Method
		Purity		Purity	
Carbon dioxide	Air Liquide	0.99995	none	-	GCa
Nitric oxide	Air Liquide	0.999	None	-	GC
Argon	Air Liquide	0.999995	None	-	GC
Oxygen	Air Liquide	0.999995	None	-	GC
Sulfur dioxide	Air Liquide	0.999	none	-	GC

a Gas chromatography

Table 2: Compositions of the two ternary systems study.

Component	Expected composition (mole fraction)	Measured composition (mole fraction) (using GC)
Mixture 1		
O <sub>2</sub>	0.03	0.0318
CO <sub>2</sub>	0.94	0.9366
Ar	0.03	0.0316
Mixture 2		



CO <sub>2</sub>	0.94	0.9205
SO <sub>2</sub>	0.03	0.0512
O <sub>2</sub>	0.03	0.0283

Table 3: Critical Properties of Pure Compounds from Reid et al. [8].

Compound	CAS number	$P_c$ / MPa	$T_c$ / K	$\omega$
O <sub>2</sub>	7782-44-7	4.977	154.58	0.0222
SO <sub>2</sub>	7446-9-5	7.884	430.75	0.2454
NO	10102-43-9	6.395	180.15	0.5829
Ar	7440-37-1	4.834	150.86	0
CO <sub>2</sub>	124-38-9	7.286	304.21	0.2236

Table 4: Vapour–liquid<sup>a</sup> equilibrium pressures and phase compositions for CO<sub>2</sub> (1) - SO<sub>2</sub> (2) mixtures ( $\sigma$ : Standard deviation between samples; n: number of samples).

$p$ /MPa	$n_x$	$x_1$	$\sigma x$	$n_y$	$y_1$	$\sigma y$
333.21 K						
1.1050		0			0	
1.4100	8	0.0296	0.0006	10	0.2080	0.002
2.080	7	0.0935	0.0008	11	0.451	0.002
2.648	6	0.1488	0.0003	13	0.563	0.008
3.241	6	0.2071	0.0002	8	0.63	0.01
3.845	6	0.2674	0.0005	8	0.6848	0.01
5.025	6	0.3892	0.0003	6	0.757	0.003
5.565	7	0.4455	0.0003	6	0.7794	0.0008
6.142	6	0.5052	0.0004	6	0.8001	0.0007
6.763	6	0.5703	0.0004	5	0.815	0.001
7.241	10	0.6195	0.0005	6	0.823	0.004
7.911	5	0.686	0.0010	6	0.836	0.002
8.544	5	0.7522	0.0002	5	0.840	0.001
8.785	5	0.7814	0.0003	6	0.8361	0.0003
263.15 K						
0.1041		0			0	
0.3554	9	0.083	0.001	6	0.742	0.003

0.5996	7	0.165	0.004	7	0.834	0.002
0.8603	8	0.260	0.003	7	0.888	0.001
1.1056	8	0.354	0.004	6	0.9222	0.0006
1.3516	8	0.460	0.005	6	0.9410	0.0003
1.6134	8	0.573	0.005	6	0.952	0.003
1.8632	7	0.687	0.004	6	0.9635	0.0006
2.0820	8	0.788	0.006	9	0.9738	0.0007
2.3495	8	0.897	0.003	6	0.9853	0.0008

<sup>a</sup>Uncertainty on temperature  $u(T, k = 2) = 0.02$  K, uncertainty on pressure  $u(P, k = 2) = 0.002$  MPa and  $u(p, k=2)=0.0002$  MPa, maximum uncertainty on composition  $u(x,y) = \pm 0.006$

Table 5: Adjusted values of binary interaction parameters of CO<sub>2</sub> (1) + SO<sub>2</sub> (2) binary system and deviations.

<i>T</i> /K	<i>k</i> <sub>ij</sub>	Bubble Pressure calculation	
		BIASP /%	AADP / %
263.15	0.0244	-0.33	1.12
333.21	0.0275	-0.57	0.78
No temperature dependency	0.0274	-0.84	1.16

Table 6: Vapour–liquid<sup>a</sup> equilibrium pressures and phase compositions for NO (1) - CO<sub>2</sub> (2) mixtures ( $\sigma$ : Standard deviation between samples; n: number of samples).

<i>p</i> /MPa	<i>n</i> <sub>x</sub>	<i>x</i> <sub>1</sub>	$\sigma$ <i>x</i>	<i>n</i> <sub>y</sub>	<i>y</i> <sub>1</sub>	$\sigma$ <i>y</i>
273.02 K						
3.505		0			0	
4.554	8	0.0318	0.0001	9	0.1656	0.0006
6.005	11	0.0790	0.0002	8	0.2948	0.0005
4.439	7	0.0284	0.0001	10	0.1514	0.0004
5.514	7	0.0626	0.0001	6	0.2605	0.0001
6.427	7	0.0925	0.0002	8	0.3192	0.0004

7.423	7	0.130	0.001	6	0.3636	0.0005
8.516	6	0.175	0.001	7	0.3897	0.0012
9.298	6	0.212	0.002	6	0.3945	0.0009
10.081	6	0.263	0.002	7	0.3806	0.0006
252.98 K						
1.9799		0			0	
2.901	10	0.0292	0.0003	7	0.2622	0.0004
4.332	10	0.0758	0.0004	8	0.450	0.0011
5.328	7	0.1117	0.0002	7	0.5168	0.0003
6.187	6	0.1441	0.0002	8	0.5535	0.0003
7.047	8	0.1781	0.0004	7	0.5787	0.0004
8.082	7	0.2229	0.0008	6	0.5988	0.0006
9.005	8	0.2666	0.0007	7	0.6062	0.0007
10.09	8	0.323	0.0014	7	0.6018	0.0006
10.992	7	0.380	0.0014	6	0.5875	0.0005
11.486	5	0.4194	0.01	7	0.5715	0.007
232.93 K						
1.0099		0			0	
1.483	7	0.0157	0.0003	6	0.2841	0.0002
2.7	7	0.0580	0.0005	6	0.5629	0.0004
3.91	6	0.1042	0.0001	6	0.6669	0.0004
4.98	6	0.1487	0.0002	6	0.7126	0.0005
5.999	6	0.1953	0.0007	6	0.739	0.001
7.008	7	0.2446	0.0005	7	0.7550	0.0003
8.013				6	0.761	0.001
8.008	6	0.2960	0.0005			
9.015				7	0.7661	0.0006
9.009	6	0.3479	0.0003			
10.073				8	0.761	0.002
10.082	10	0.409	0.002			
11.214				7	0.743	0.005
11.208	10	0.473	0.001			

<sup>a</sup>Uncertainty on temperature  $u(T, k = 2) = 0.02$  K, uncertainty on pressure  $u(P, k = 2) = 0.002$  MPa and  $u(p, k=2)=0.0002$  MPa, maximum uncertainty on composition  $u(x,y) = \pm 0.006$

Table 7: Adjusted values of binary interaction parameters of NO (1) + CO<sub>2</sub> (2) binary system and deviations.

$T/K$	$k_{ij}$	Bubble Pressure calculation	
		BIASP /%	AADP / %
273.15	-0.0925	0.9	1.9
252.98	-0.1009	6.6	6.6
232.93	-0.0071	-1.8	5.9
No temperature dependency	-0.0323	-2.3	6

Table 8: Vapour–liquid<sup>a</sup> equilibrium pressures and phase compositions for CO<sub>2</sub> (1) + Ar (2) + O<sub>2</sub> (3) (mixture 2, 0.9366/0.0316/0.0318) mixtures ( $\sigma$ : Standard deviation between samples; n: number of samples).

$T/K$	$p/MPa$	$n_x$	$x_{CO_2}$	$x_{Ar}$	$\sigma_{xCO_2}$	$\sigma_{xAr}$	$n_y$	$y_{CO_2}$	$y_{Ar}$	$\sigma_{yCO_2}$	$\sigma_{yAr}$
253.28	2.327	4	0.9911	0.0043	0.0003	0.0002	4	0.8674	0.0654	0.0007	0.0002
253.28	2.666	5	0.9839	0.0079	0.0004	0.0002	4	0.7728	0.1125	0.0007	0.0003
253.28	3.001						4	0.7007	0.1486	0.0005	0.0003
253.28	2.999	4	0.9765	0.0115	0.0003	0.0001					
253.27	3.351						4	0.6435	0.1771	0.0004	0.0009
253.27	3.350	4	0.9685	0.0154	0.0005	0.0003					
253.27	3.709						4	0.5927	0.2029	0.002	0.0008
253.27	3.715	4	0.9599	0.0198	0.0005	0.0003					
253.27	4.033						4	0.5550	0.2214	0.003	0.003
253.27	4.031	4	0.9515	0.0240	0.0004	0.0002					
253.27	4.215						4	0.536	0.230	0.002	0.001
253.27	4.213	4	0.9466	0.0263	0.0003	0.0002					
273.26	4.096	2	0.9843	0.0076	0.0002	0.0002	3	0.8901	0.0541	0.0002	0.0006
273.24	4.368	2	0.9778	0.0109	0.0007	0.0002	3	0.853	0.073	0.004	0.002
273.24	4.679						4	0.810	0.0942	0.001	0.0007
273.24	4.678	4	0.9707	0.0142	0.0004	0.0001					
273.24	5.022						5	0.771	0.1129	0.001	0.0008
273.24	5.021	4	0.9626	0.0184	0.0005	0.0002					
273.24	5.311						5	0.744	0.127	0.002	0.002
273.24	5.309	4	0.9547	0.0227	0.0004	0.0004					
273.24	5.673						4	0.714	0.1418	0.002	0.0007
273.24	5.670	4	0.9451	0.0271	0.0005	0.0001					
293.21	6.590	5	0.9751	0.0122	0.0003	0.0002	4	0.9208	0.0395	0.0009	0.0002
293.21	6.827	5	0.9692	0.0151	0.0004	0.0004	5	0.9047	0.0471	0.0008	0.0006
293.21	7.113						4	0.887	0.0559	0.001	0.0005
293.22	7.112	5	0.9609	0.0193	0.0002	0.0002					
293.21	7.340	5	0.9530	0.0233	0.0008	0.0004	4	0.875	0.0619	0.001	0.0004
293.21	7.638	4	0.942	0.0285	0.001	0.0005	4	0.862	0.068	0.003	0.002

<sup>a</sup>Uncertainty on temperature  $u(T, k = 2) = 0.02$  K, uncertainty on pressure  $u(P, k = 2) = 0.002$  MPa and  $u(p, k=2)=0.0002$  MPa, maximum uncertainty on composition  $u(x,y) = \pm 0.002$

Table 9: Vapour–liquid<sup>a</sup> equilibrium pressures and phase compositions for O<sub>2</sub> (1) - CO<sub>2</sub> (2) + SO<sub>2</sub> (3) (mixture 2, 0.0283/0.9205/0.0512) mixtures ( $\sigma$ : Standard deviation between samples; n: number of samples).

<i>T</i> /K	<i>p</i> /MPa	<i>n<sub>x</sub></i>	<i>x</i> O2	<i>x</i> CO2	$\sigma$ xO2	$\sigma$ xCO2	<i>n<sub>y</sub></i>	<i>y</i> O2	<i>y</i> CO2	$\sigma$ yO
293.24	5.207	7	0.00573	0.88218	0.00002	0.0004	8	0.03491	0.93250	0.0000
293.24	5.301	7	0.00642	0.89128	0.00003	0.0002	8	0.0375	0.9323	0.0000
293.23	5.397	8	0.00726	0.89955	0.00002	0.0002	6	0.0399	0.9321	0.0000
293.23	5.494	9	0.00819	0.90611	0.00003	0.0002	8	0.0435	0.9303	0.0000
293.23	5.601	7	0.00944	0.91240	0.00002	0.0001	6	0.04789	0.92776	0.0000
293.23	5.712	6	0.01095	0.91692	0.00002	0.0004	6	0.05331	0.92416	0.0000
293.23	5.841	8	0.01296	0.92038	0.00002	0.0001	8	0.0606	0.9181	0.0000
293.23	5.966	7	0.01516	0.92221	0.00004	0.0002	7	0.0680	0.9117	0.0000
293.23	6.088	6	0.01741	0.92301	0.00003	0.0002	9	0.0748	0.9058	0.0000
293.23	6.257	6	0.02080	0.92273	0.00004	0.0002	6	0.0855	0.8958	0.0000
293.23	6.382	6	0.02331	0.92177	0.00005	0.0001	7	0.0930	0.8885	0.0000
293.23	6.473	6	0.02530	0.92109	0.00004	0.0001	6	0.0981	0.8835	0.0000
273.26	3.333	8	0.00404	0.90369	0.00003	0.0004	7	0.04798	0.93613	0.0000
273.26	3.425	7	0.00497	0.91268	0.00004	0.0005	7	0.0557	0.9301	0.0000
273.27	3.577	6	0.00695	0.92268	0.00005	0.0003	6	0.07292	0.91508	0.0000
273.26	3.747	7	0.00972	0.92698	0.00003	0.0004	7	0.0962	0.8931	0.0000
273.26	3.823	7	0.01099	0.92760	0.00008	0.0006	6	0.1066	0.8832	0.0000
273.26	3.962	7	0.01345	0.92765	0.00008	0.0005	7	0.1255	0.8647	0.0000
273.26	4.091	6	0.0159	0.9269	0.0001	0.0004	7	0.1413	0.8492	0.0000
273.26	4.200	7	0.0179	0.9262	0.0001	0.0005	7	0.1554	0.8355	0.0000
273.26	4.364	6	0.0211	0.9244	0.0001	0.0006	6	0.1743	0.8169	0.0000
273.27	4.517	6	0.0242	0.9224	0.0002	0.0002	9	0.1913	0.8000	0.0000
253.28	1.935	7	0.00247	0.91097	0.00007	0.002	7	0.05862	0.93321	0.0000
253.28	2.098	7	0.0047	0.9289	0.0001	0.0005	7	0.0991	0.8948	0.0000
253.28	2.249	6	0.00724	0.93231	0.00008	0.0008	6	0.14080	0.85366	0.0000
253.29	2.466	6	0.01105	0.93216	0.00009	0.0002	7	0.19626	0.79876	0.0000
253.28	2.657	6	0.0145	0.9306	0.0002	0.0003	6	0.23924	0.75607	0.0000
253.28	2.814	7	0.01733	0.92862	0.00005	0.0004	7	0.27052	0.72499	0.0000
253.28	2.912	8	0.0190	0.9270	0.0002	0.0005	11	0.287	0.709	0.002
253.28	3.022	9	0.02109	0.92549	0.00009	0.0005	9	0.30559	0.69030	0.0000
253.28	3.126	8	0.0231	0.9239	0.0002	0.0005	9	0.32264	0.67329	0.0000

<sup>a</sup>Uncertainty on temperature  $u(T, k = 2) = 0.02$  K, uncertainty on pressure  $u(P, k = 2) = 0.002$  MPa and  $u(p, k=2)=0.0002$  MPa, maximum uncertainty on composition  $u(x,y) = \pm 0.005$

Table 10: Data treatment of literature data using PR EoS (BIP and deviations using bubble point calculation).

Binary system	(BIP) $k_{ij}$ value	Bubble point calculation	
		BIAS P /%	AAD P/%
CO <sub>2</sub> + Ar	0.1060	1.4	4.1
CO <sub>2</sub> + O <sub>2</sub>	0.1053	1.6	4.7
Ar + O <sub>2</sub>	0.0126	-0.05	0.3
SO <sub>2</sub> + O <sub>2</sub>	0.2336	-3.1	4.5

Table 11: Ternary systems: deviations between experimental and predicted values.

Mixture	BIAS x or y/%						$x_1$	$x_2$	$x_3$
	$x_1$	$x_2$	$x_3$	$y_1$	$y_2$	$y_3$			
1	0.1	-2.1	-0.3	-1.9	5.6	7.5	0.1	3.0	2.3
2	-4.7	0.1	-0.4	-6.7	1.7	5.7	4.7	0.2	1.8

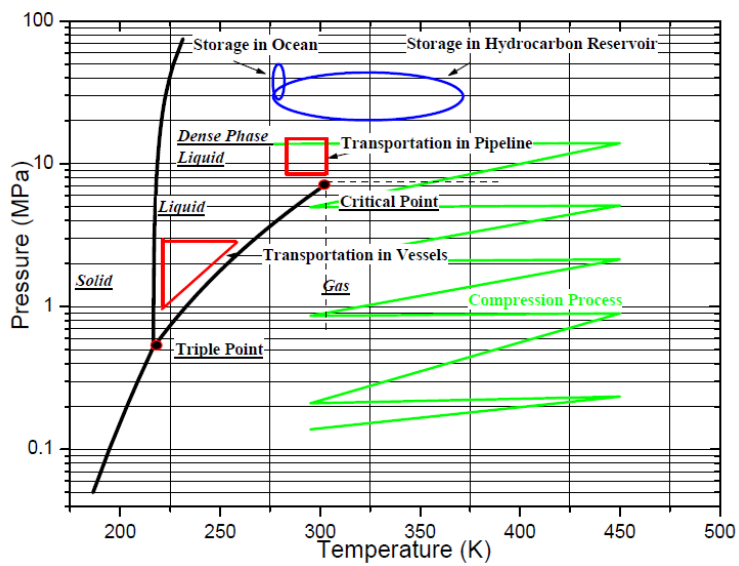


Figure 1

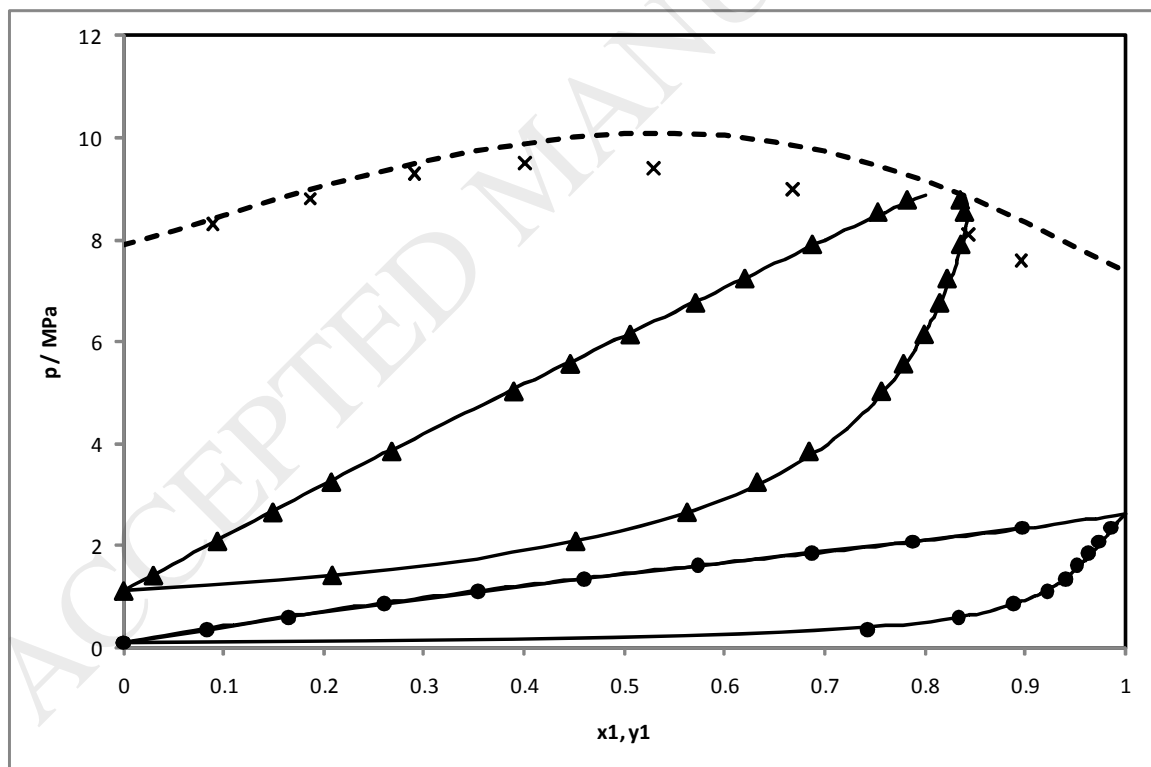


Figure 2

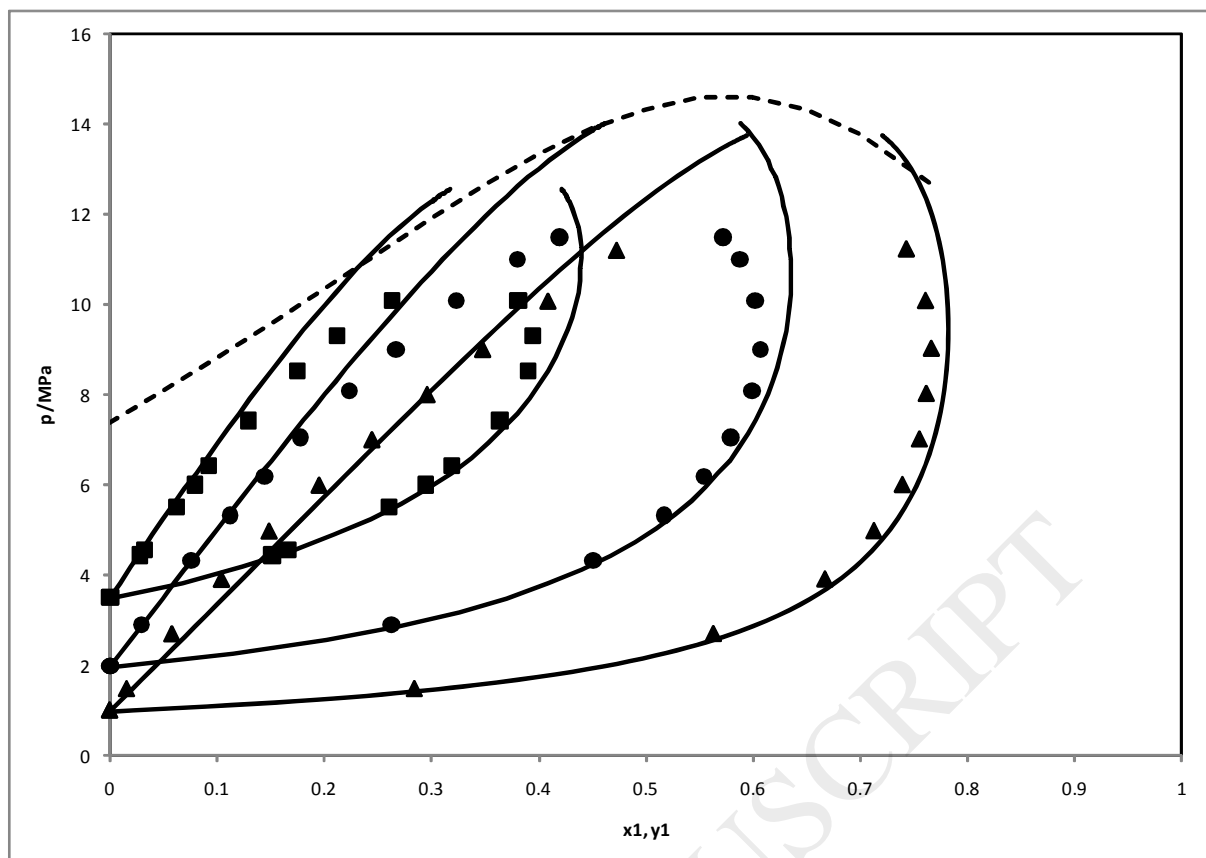


Figure 3

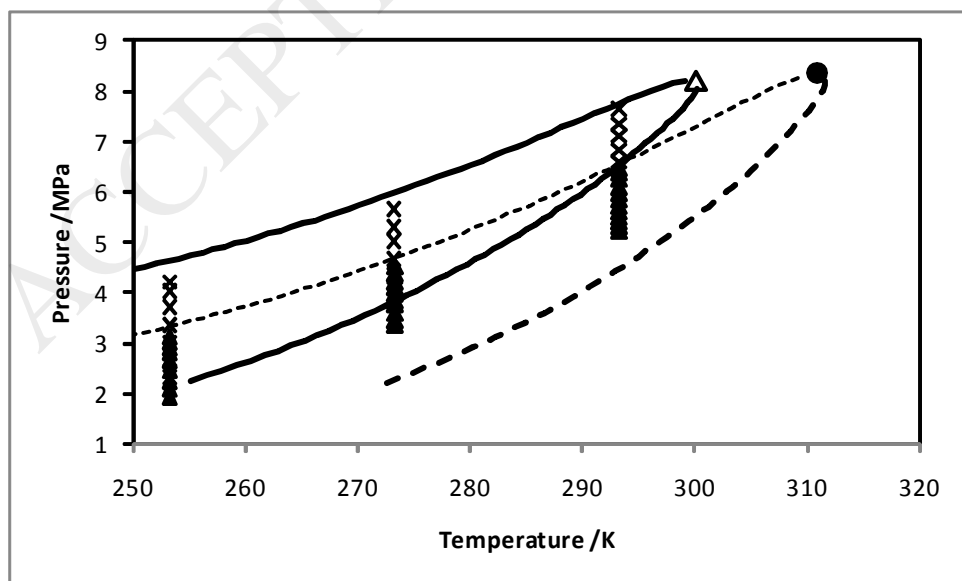




Figure 4

ACCEPTED MANUSCRIPT